Research Article

Lijuan Tan*

Curcumin conjugated zinc nanoparticles for the treatment of myocardial infarction

https://doi.org/10.1515/chem-2024-0051 received December 11, 2023; accepted June 1, 2024

Abstract: A modern cardioprotective drug was created by utilizing zinc nanoparticles (ZnNPs) containing curcumin to address isoproterenol-induced myocardial infarction in mice, with a specific focus on the PPAR-γ/NF-κB pathway. During the in vivo study, mice were subjected to myocardial infarction by subcutaneously administering isoproterenol at a dosage of 40 mg/kg every 12 h for a total of three administrations. The mice were randomly divided into five groups: (I, II) isoproterenol + ZnNPs at different concentrations (10, 40 µg/mL) and time intervals, (III) isoproterenol alone, and (IV) control group. Various physicochemical methods, including FT-IR, field emission scanning electron microscopy, X-Ray diffraction analysis, fourier-transform infrared spectroscopy and energy dispersive X-ray spectroscopy, were utilized to analyze and characterize the ZnNPs. The real-time PCR and western blot methods were used to examine the PPAR-y/NF-κB activation by lipopolysaccharide (LPS) and the subsequent cytokine release. This research focused on investigating the inflammatory responses and cell apoptosis in human coronary artery endothelial cells treated with LPS. After the therapy, cardiac function was checked using an electrocardiogram, along with biochemical and histochemical analysis. The introduction of ZnNPs leads to a decrease in the inflammatory conditions present in the hearts of mice suffering from myocardial infarction. The use of ZnNPs not only enhances ventricular wall infarction but also reduces mortality rates and suppresses levels of myocardial injury markers. The usual ST segment depression observed in mice with myocardial infarction is markedly reduced when treated with ZnNPs. The mice with myocardial infarction in the pre + post-isoproterenol group seemed to experience more pronounced cardioprotective effects from the treatment with ZnNPs compared to those in the post-isoproterenol group. In an in vitro experiment, the use of ZnNPs resulted in a

significant reduction in cell death and inhibition of inflammation cytokine expression. The gene expression normalization for PPAR-γ/NF-κΒ/ΙκΒ-α/ΙΚΚα/β and the phosphorylation of PPAR-γ could potentially be associated with the beneficial effects of ZnNPs. The rise in inflammatory responses was effectively prevented. The results of this study indicate that ZnNPs have cardioprotective efficacies on isoproterenol-induced myocardial infarction. This positive impact could be linked to the PPAR-γ activation and the NF-κB signaling inhibition.

Keywords: curcumin, myocardial infarction, NF- κ B, PPAR- γ , zinc nanoparticles

1 Introduction

Ischemic heart disease poses a significant public health concern due to its increasing burden. Acute myocardial infarction results in tissue loss and compromised heart function, contributing to 40% of deaths in China [1]. Timely revascularization following a heart attack, such as bypass surgery, thrombolytic therapy, and percutaneous coronary intervention, plays a crucial role in enhancing heart function and averting post-heart attack physiological changes [2]. Nevertheless, these efficient yet intrusive methods may not be suitable for every patient due to their limited applicability dependent on particular clinical traits, as well as the potential for severe complications like reperfusion injury and bleeding [2,3]. Efforts to reduce infarct size and enhance prognosis through pharmacotherapy (such as angiotensinconverting enzyme inhibitors) in the absence of reperfusion are mainly ineffective, primarily due to non-specific drug delivery, adverse effects, and the brief duration of action of certain drugs [1-4]. As a result, numerous patients undergoing this method continue to develop heart failure and cardiac hypertrophy [1,2]. The atherosclerotic plaques rupture and growth, leading to thrombosis, are the primary factors contributing to acute myocardial infarction [4]. Presently, the interventions accessible for atherosclerosis, such as statins, can lower the acute myocardial infarction risk. However, the impact of these interventions differs among

^{*} Corresponding author: Lijuan Tan, Department of Cardiac Intensive Care Unit, Shanxi Cardiovascular Hospital, Taiyuan, Shanxi Province, 030024, China, e-mail: lijuantan77@sina.com

individuals, resulting in notable residual risks [5–8]. Certain chemotherapies, like methotrexate and docetaxel, appear to exhibit advantageous outcomes in atherosclerosis [9–11]. Nevertheless, the drugs administration systemically is restricted due to their unfavorable efficacies. The need for safer and more effective prevention and treatments methods for myocardial infarction is on the rise [12].

Nanotechnology is instrumental in the progress of contemporary treatment alternatives [13,14]. It facilitates the creation and tailoring of materials possessing exceptional properties and attributes, spanning from 1 to 100 nm in size [13]. Currently, a diverse range of nanoparticles are produced through chemical or physical methods. Nevertheless, the utilization of hazardous chemicals and the subsequent environmental damage have given rise to multiple apprehensions [14–16]. Nanoparticles are receiving increased attention due to their importance in biology and potential uses in medicine. Nevertheless, the traditional chemical techniques utilized in their creation frequently introduce harmful reactive materials, making the produced nanoparticles unsuitable for medical applications. The adoption of environmentally friendly methods in nanoparticle production has been extensively acknowledged in several scientific studies [14–16], solidifying its status as a key research focus. Plant extracts have shown great potential as an alternative method for producing metal oxide NPs compared to traditional approaches. The versatility of NPs in fields like medicine, industry, and agriculture is extensive, highlighting their importance across various sectors [17-19]. Researchers have recently been drawn to the unique efficacies and diverse applications of nanoparticles. These minuscule particles have proven to be helpful in a wide array of areas including biological markers, optoelectronic catalysts, medical treatments, and pharmaceuticals. Furthermore, the use of plants to synthesize nanoparticles on a larger scale presents additional benefits, such as the capacity to reduce and absorb metal ions [16–19].

Numerous therapeutic optimized approaches have been extensively investigated, among them being the utilization of nanoparticles. These minute particles at the nanoscale have found significant application in managing both tumors and neural disorders [16–20]. Nanoparticles facilitate the transportation of therapeutic substances to specific locations with precise spatial and temporal accuracy, improve tissue engineering procedures efficiency, and control the activities of transplants like stem cells [16–19]. Utilizing nanoparticles enhances the efficacy of treatments and reduces the negative impacts of conventional or innovative therapies, enhancing the probability of their successful implementation in clinical environments. Nevertheless, studies on NPs in this area are still in the early stages [13–15].

Zinc nanoparticles (ZnNPs) are noteworthy because of their chemical and physical properties. Additionally, ZnNPs have gained traction in biological uses thanks to their minimal toxicity levels. ZnNPs play a beneficial role in biomedicine, specifically in combating fungal infections, bacterial infections, cancer, and diabetes [21–23]. Furthermore, ZnNPs exhibited anti-inflammatory, antioxidant, and hypolipidemic characteristics [24,25]. Zinc has a main role in maintaining the function and structure of cell membranes, defending against pathogens, enhancing brain function, promoting tissue development, and supporting immunity [26,27]. Additionally, ZnNPs are utilized in the present for their capacity to load drugs, ability to release drugs in a controlled manner, and targeted delivery capabilities [28]. Furthermore, zinc plays essential roles in the formation and operation of various antioxidant enzymes and distinct metallothioneins [29]. In the cardiovascular diseases development, including ischemic cardiomyopathy, myocardial infarction, and coronary heart disease, the fluctuation in Zn homeostasis plays a significant role, potentially contributing to cardiovascular diseases mortality [30].

In this study, the main objective is to create ecofriendly ZnNPs using curcumin. The author conducted a thorough analysis of the ZnNPs by employing microscopic imaging, diffraction, and spectroscopic techniques to gain insights into their size, shape, and structure. Additionally, the author assessed the therapeutic effects of these ZnNPs in the myocardial infarction treatment.

2 Materials and methods

2.1 Preparation of curcumin

To obtain curcumin from turmeric, the initial step involved cutting the turmeric rhizomes into small pieces (0.5–1 cm) and washing them with water. Subsequently, curcumin was extracted from the turmeric pieces (10 g) using a Soxhlet apparatus. A solvent extract of 100 mL of water: ethanol (1:1) was utilized for this purpose. Following a 4 h extraction period, the extract was cooled down before being employed in nanoparticles synthesis.

2.2 Green formulation of ZnNPs

To create the 0.04 M zinc nitrate stock solution, the curcumin (50 mL) was combined with the zinc nitrate stock solution (20 mL) and incubated for 180 min at 25°C. A noteworthy change in color was subsequently reported. The ZnNPs biosynthesis was confirmed by transmission electron microscopy (TEM), ultraviolet—visible spectroscopy (UV-Vis), field emission scanning electron microscopy (FE-SEM), X-Ray diffraction analysis (XRD), fourier-

transform infrared spectroscopy (FT-IR) and Energy dispersive X-ray spectroscopy (EDX) [13–15].

2.3 Chemical characterization of ZnNPs

UV-Vis analysis was conducted to check the nanoparticles absorbance value within the 200-600 nm range. The biogenic ZnNPs surface plasmon resonance (SPR) was recorded using the UV-Vis spectrophotometer.

FE-SEM was utilized for the examination of the structure and makeup of ZnNPs. The ZnNPs size distribution was depicted in a histogram through image software.

The identification of the various functional groups accountable for the stabilization and reduction of the formulated ZnNPs was accomplished through FT-IR analysis, utilizing the Cary 630 FTIR model from Tokyo, Japan. It was conducted using the KBr technique.

The XRD has verified that the synthesized NPs are ZnNPs. Following the synthesis of ZnNPs, the samples underwent centrifugation in preparation for the XRD analysis. The X-ray analysis involved adjusting the angle every 3.4 s for a total of three steps, with each step lasting 34 s.

TEM analysis was employed to investigate the structure of ZnNPs using a JEOL model JEM-1010 from Tokyo, Japan.

The Shimadzu DX-700HS machine was utilized to conduct an EDX analysis to identify the elements.

The Zetasizer nano-array was employed to determine the zeta potential. The measurements were conducted at dispersion angles of 90 and 25°C.

2.4 In vivo experimental design

During this experimental investigation, a total of 75 male BALB/c mice weighing between 38 and 40 g were utilized. The mice was housed in a controlled setting with a temperature maintained between 20 and 24°C. It is important to highlight that all procedures conducted in this study adhered to ethical guidelines concerning the use of laboratory animals.

- I) Myocardial infarction + ZnNPs (10 μg/kg).
- II) Myocardial infarction + ZnNPs (40 μg/kg).
- III) Myocardial infarction + curcumin.
- IV) Myocardial infarction group.
- V) Control group.

After the mice were accustomed to their surroundings, myocardial infarction was triggered in the mice by injecting isoproterenol (85 mg/kg) dissolved in normal saline (1 mg/mL) subcutaneously for 2 consecutive days with a 24 h gap, following the procedure described in the earlier research. (The next day, four animals exhibited shedding, leading to their immediate replacement.) The standard protocols were utilized to establish the induction of myocardial infarction. Following that, a group of mice were anesthetized 48 h after the occurrence of myocardial infarction, and samples of heart tissue from their left ventricle were examined using hematoxylineosin histochemical techniques. The identification of white areas indicated necrotic damage caused by the heart attack [31].

After the final administration of isoproterenol, the mice underwent anesthesia. The researchers then assessed the presence of ST-segment depression or elevation in the animals. On the fifth day, the mice were euthanized to analyze the immunological and biochemical factors. ELISA kits were used to determine the expression levels of IL-6, IL-1β, and TNF-α in the homogenized left ventricular heart tissues supernatant. The myocardial cellular damage extent was determined by examining the levels of serum troponin and creatinine kinase isoenzyme. Additionally, an ELISA assay was utilized to measure the levels of serum creatinine kinase isoenzyme and troponin [31].

The Qiasol kit (Qiagen) was used to extract the RNA from the examined heart, following the instructions provided. The concentration of the isolated RNA was assessed using a nanodrop spectrophotometer. The optical absorption of the samples was quantified at a wavelength of 280 nm, with the concentration being calculated according to the dilution factor in μL/ng. Next, a 1 ng/μL RNA solution was prepared for cDNA synthesis. To achieve this, 10 µL of a cDNA synthesis kit was mixed with 10 µL of RNA. The mixture was subsequently placed in a thermocycler and incubated at 25°C for 10 min, followed by 60°C for 50 min. Finally, the resulting cDNA was stored for qPCR analysis at -20°C. The gene replication rate was investigated through the performance of PCR. The control gene utilized in this research was the beta-actin gene. The temperature program for amplifying the PPAR/GAPDH gene, including PPARy/NF-κΒ/ΙκΒ-α/ΙΚΚα/β, PPAR-y, and β-actin, consisted of a series of steps. These steps included primary denaturation for 4 min at 94°C, followed by secondary denaturation at 94°C for 1 min. The temperature was initially set at 55°C for 1 min for the binding process, followed by primary synthesis for 1 min at 52°C. This cycle was repeated 40 times, covering steps 2-4, and concluded with the final synthesis for 18 min at 52°C. Subsequently, the obtained graphs were analyzed to determine changes in gene expression through $\Delta\Delta$ CT analysis, based on the CT variance among the different intervention groups [14,31] (Table 1).

2.5 Statistical analysis

The normality of the data was assessed using Minitab-21 in the research. Following this, any data that was not

Table 1: Primer sequences of genes studied in this research

Gene	Sequence	GenBank		
β-actin	Forward: CACCATTGGCAATGAGCGGTTC	NM_001101		
	Reverse: AGGTCTTTGCGGATGTCCACGT			
PPAR-y	Forward: AGCCTGCGAAAGCCTTTTGGTG	NM_015869		
	Reverse: GGCTTCACATTCAGCAAACCTGG			
ΙκΒ-α	Forward: TCCACTCCATCCTGAAGGCTAC	NM_020529		
	Reverse: CAAGGACACCAAAAGCTCCACG			
NF-kB p65	Forward: TGAACCGAAACTCTGGCAGCTG	NM_021975		
	Reverse: CATCAGCTTGCGAAAAGGAGCC			

normally distributed was transformed to achieve normality. The data variance analysis was done with SPSS-22, and graphical illustrations were generated using Excel software.

3 Results and discussion

3.1 Chemical characterization

The metal–oxygen bond is associated with bands below 700 cm⁻¹ in FT-IR analysis. In Figure 1 of the FT-IR spectrum of ZnNPs, the Zn–O bond is represented by bands at 458 and 523 cm⁻¹. The additional peaks at 1,056, 1,381–1,633, 2,958, and 3,428 correspond to the organic functional groups of curcumin, which serve as the reducing agent during the synthesis process.

EDX assay is the practical method for nanoparticles elemental screening. The EDX diagram and elemental mapping of nanoparticles are reported in Figures 2 and 3. The energy signals at 8.6 and 9 keV are designated for Zn L α and Zn K β , respectively. The presence of signals at 0.52 (O L α) and 0.27 (for C L α) confirms the secondary metabolites connection from the extract to the synthetic ZnNPs surface.

One technique utilized to characterize metal nanoparticles involves examining electron microscope (FE-SEM) image, which are useful for analyzing the morphology of the produced NPs. The TEM and FE-SEM images captured from ZnNPs under the specified ideal parameters reveal the production of spherical nanomaterials (Figures 4 and 5). The particles that were generated had a size of 10–60 nm. On average, the nanoparticles that were synthesized had a size between 10 and 30 nm. In terms of their morphology, the nanoparticles exhibited crystalline geometric and uniform shapes. Additionally, due to the lengthy waiting time for analysis, the ZnNPs tended to agglomerate to some extent.

The mixture of plant extract and zinc nitrate salt was combined and left to incubate for 180 min. Throughout this period, a noticeable alteration in color occurred within the reaction mixture. The initial yellow-orange hue of the solution transformed into a deep brown shade, thereby approving the phytosynthesis occurrence in the ZnNPs production. The color change was a consequence of the nanoparticles' exhibited SPR activity [22,25]. The color intensity is dictated by the electrons quantity liberated during the conversion of NO₃ to NO₂, leading to the Zn⁺⁺ reduction to metallic ions [24,25]. The research the author conducted was backed by the results from previous studies [22,25], which mirrored the findings regarding the visual alteration of the solution's color. Further investigation into the reaction solution color change was conducted by analyzing the ZnNPs UV-Vis spectrum. An absorption peak at 282 nm was reported in the ZnNPs, which was attributed to the free electrons excitation of the metal during

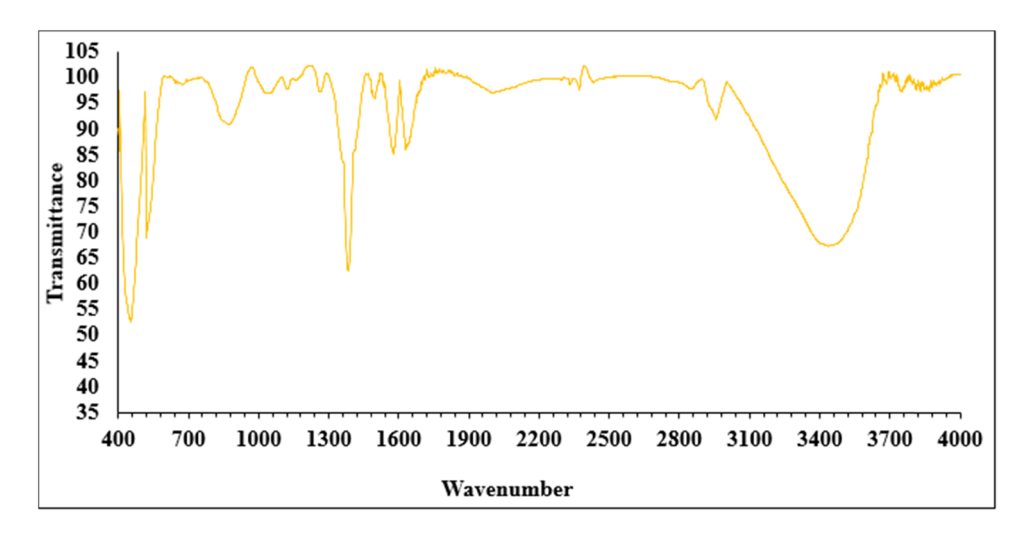


Figure 1: FT-IR analysis of ZnNPs green-mediated by curcumin.

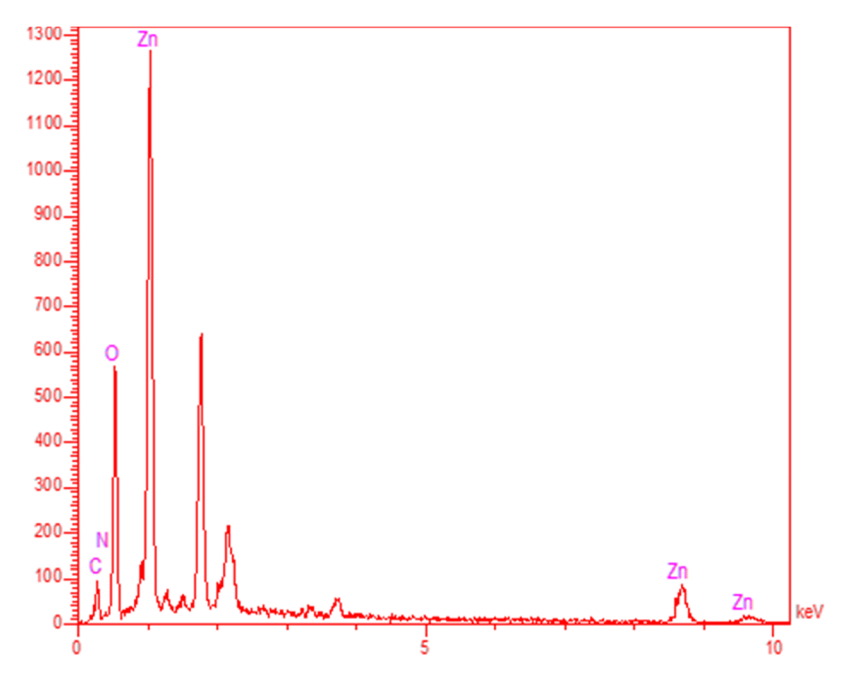
the nanoparticles formation (Figure 6). Nevertheless, the absorption peak absence was observed in the plant extract within this particular range. Typically, these spectra offer valuable insights into the characteristics and development of colloidal ZnNPs. An absorption peak between 200 and 300 nm is a distinctive attribute of ZnNPs [25–29].

ZnO colloidal particles exhibit a neutral charge at their isoelectric point (pI). When the pH is below the pI of ZnO, the particles acquire a positive charge, which hinders their aggregation and leads to the formation of a stable suspension. Likewise, when the pH exceeds the pI of ZnO, the particles become negatively charged on the surface, resulting in similar observations. Figure 7 illustrates the standard relationship between pH and the zeta potential of ZnO suspension. The zeta potential becomes positive in acidic conditions. The isoelectric point (pI) is approximately at pH 9.9. The surface area is intricately linked to the size and morphology of the particles [32].

Figure 8 displays the XRD diffraction diagrams of ZnNPs, indicating the successful crystallization of the nanoparticles. The results have been compared to the ICDD PDF card no. 01-080-3002 for validation. The peaks observed at 2θ angles of 67.98, 62.86, 56.62, 47.59, 36.15, 34.48, and 31.82 correspond to the crystal planes of (112), (103), (110), (102), (101), (002), and (100). The crystal size of ZnNPs was determined to be 19.52 nm using Scherer's equation.

3.2 Cardioprotective effects of ZnNPs greenmediated by curcumin

A recent investigation involved the administration of isoproterenol to mice to induce myocardial infarction. Elevated doses of isoproterenol quickly increase the myocardial



Elt	Line	Int	Error	К	Kr	W%	Α%	ZAF	Ox %	Pk/Bg	Class	LConf	HConf	Cat#
С	Ka	40.0	3.8197	0.0618	0.0359	15.25	28.54	0.2355	0.00	6.16	Α	13.74	16.77	0.00
N	Ka	3.3	3.8197	0.0066	0.0038	1.43	2.30	0.2672	0.00	2.30	В	0.94	1.93	0.00
О	Ka	329.5	3.8197	0.2923	0.1699	38.19	53.65	0.4448	0.00	18.45	Α	36.87	39.51	0.00
Zn	Ka	111.6	0.7275	0.6393	0.3715	45.12	15.51	0.8234	0.00	11.44	Α	42.44	47.80	0.00
				1.0000	0.5812	100.00	100.00		0.00					0.00

Figure 2: EDX analysis of ZnNPs green-mediated by curcumin.

6 — Lijuan Tan DE GRUYTER

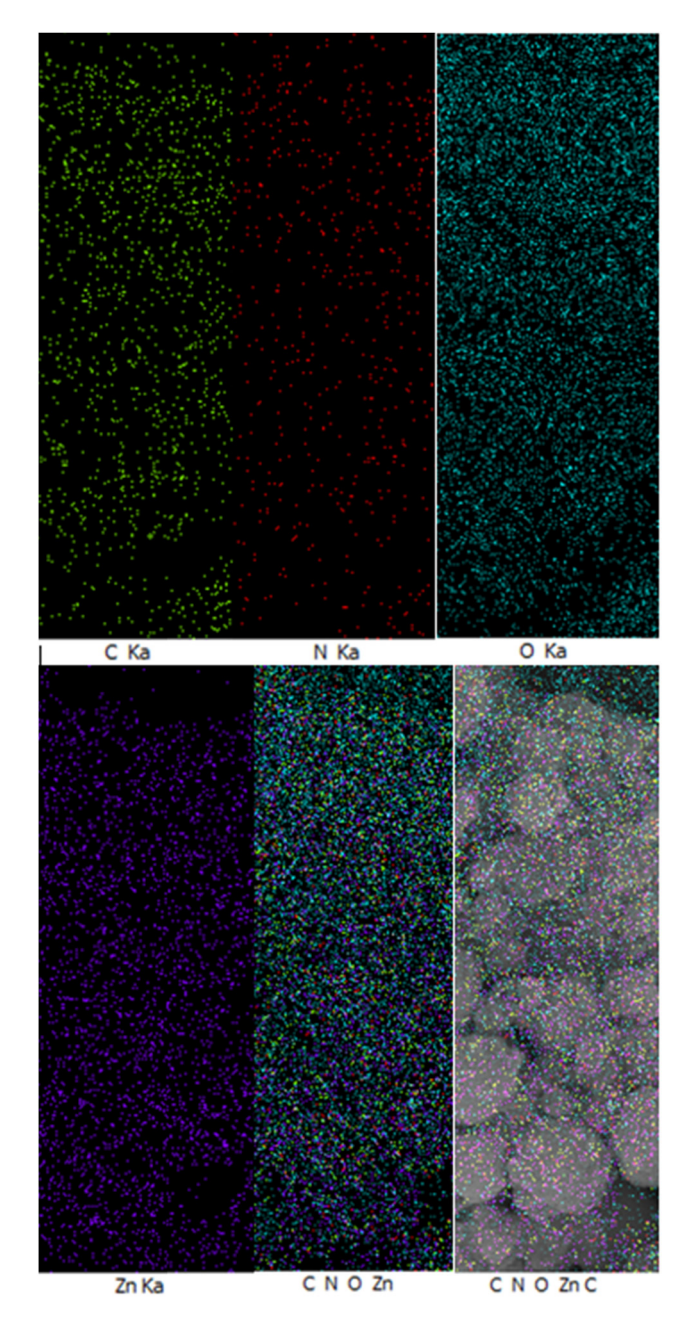


Figure 3: Elemental mapping analysis of ZnNPs green-mediated by curcumin.

load, resulting in myocardial dysfunction. The changes in morphology and pathophysiology induced by isoproterenol in mice closely mirror those seen in human myocardial infarction. Increased free radicals production during myocardial infarction leads to heightened activity of the MAPK signaling pathway, which includes three subfamilies: p38, JNK, and ERK. Activation of this pathway boosts κ B-NF, leading to an increase in inflammatory cytokines production and ultimately causing damage to the myocardium [33]. Extensive studies have been done on the ERK signaling

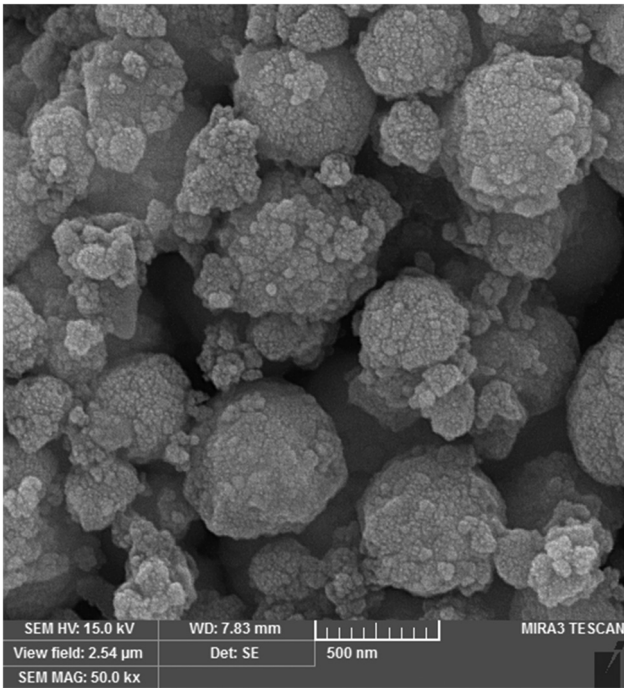


Figure 4: FE-SEM image of ZnNPs green-mediated by curcumin.

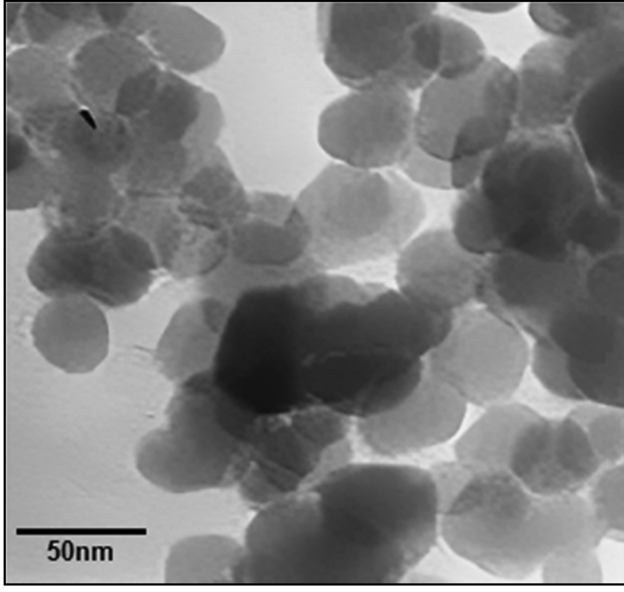


Figure 5: TEM image of ZnNPs green-mediated by curcumin.

pathway, which is crucial in regulating cellular death, growth, and survival, along with the immune response linked to inflammation [34]. Despite the association of p38 MAPK and JNK with apoptosis, the importance of ERK lies in its role in promoting cell survival and minimizing the chances of myocardial infarction [35]. Numerous research reported the involvement of κB -NF and MAPK pathways in myocardial

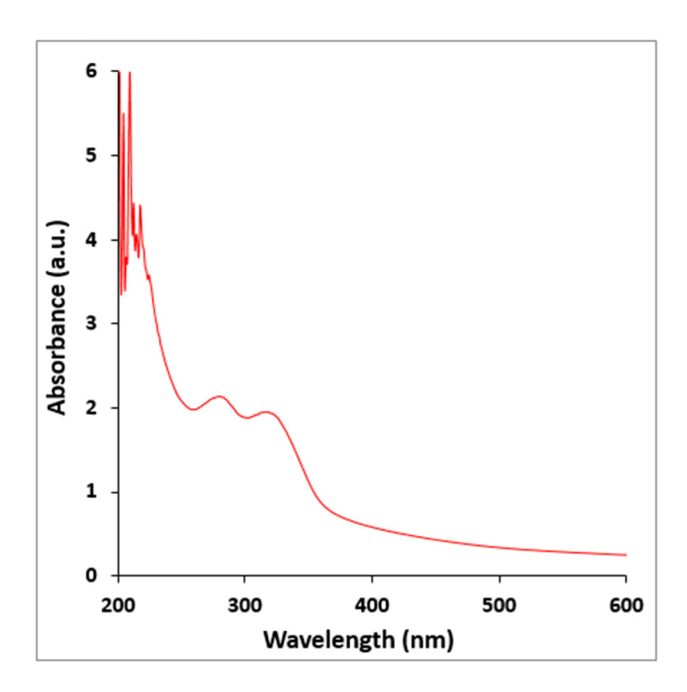


Figure 6: UV-Vis analysis of ZnNPs green-mediated by curcumin.

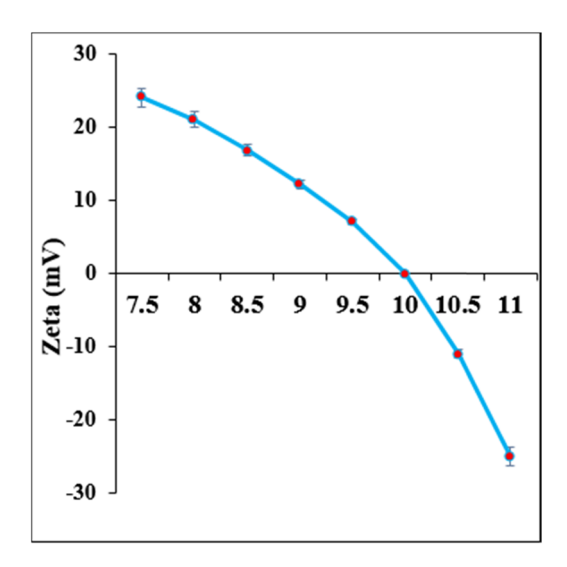


Figure 7: Zeta potential values of ZnNPs green-mediated by curcumin at several pH values (at 25°C).

hypertrophy, heart failure, and blood pressure regulation. Several research findings have indicated that the inhibition of MAPK can lead to the 2-Nrf activation, which plays a critical role in regulating the expression of antioxidant and detoxification enzymes during the second step [34–36].

The study introduced an eco-friendly formulation of ZnNPs synthesized using curcumin. Different spectroscopic methods were utilized to analyze the ZnNPs, and their potential in treating myocardial infarction was explored.

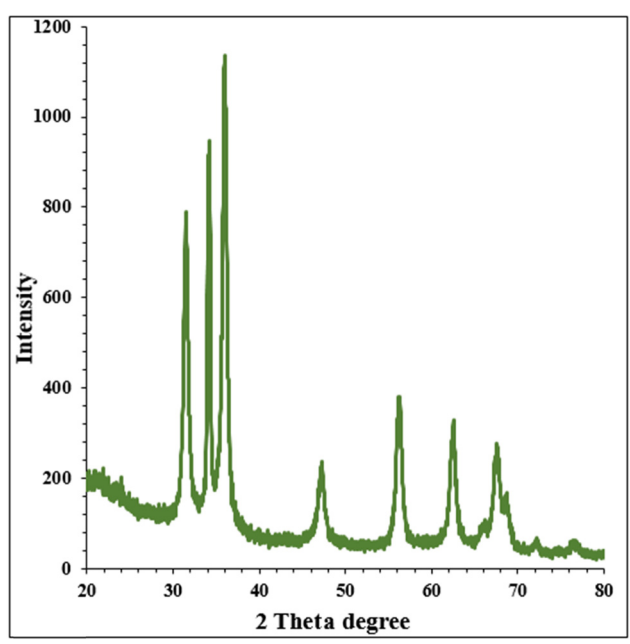


Figure 8: XRD analysis of ZnNPs green-mediated by curcumin.

The present study examined the protective properties of nanoparticles derived from curcumin in preventing myocardial damage. This was done by creating a myocardial infarction model in mice using isoproterenol. Additionally, the research evaluated the expression levels of PPAR-y/NFκΒ/ΙκΒ-α/ΙΚΚα/β, and PPAR-y or MAPK signaling pathway in the experimental groups to gain insight into the treatment's mechanism (Figure 9). The green-synthesized curcumin ZnNPs resulted in a decrease in the levels of p-IKKα/β/ IKKα/β, p-IkBα/IkBα, and p-NF-kβ p65/NF-kβ p65, along with a decline in PPAR/GAPDH. Additionally, the curcumin-derived ZnNPs produced through green synthesis showed a notable decrease ($P \le 0.05$) in the mRNA levels of IL6, TNFα, and IL1β, as well as the presence of CD68⁺ cells, in comparison to the control group (Figure 10). The mice involved in the study displayed a model of myocardial infarction induced by isoproterenol. This was supported by the significant accumulation of collagen and extensive damage to the myocardial tissue. Additionally, the expression of MAPK was found to be increased, providing further validation of the model's effectiveness. Recent research has proposed that various signaling pathways, including the proteins within the MAPK pathway, change in response to myocardial damage caused by isoproterenol [37]. Recent studies have shown that isoproterenol is effective in boosting MAPK levels. The MAPK pathway plays a key role in controlling gene expression related to apoptosis, such as Bax and Bcl-2. These genes are essential components of the apoptotic signaling

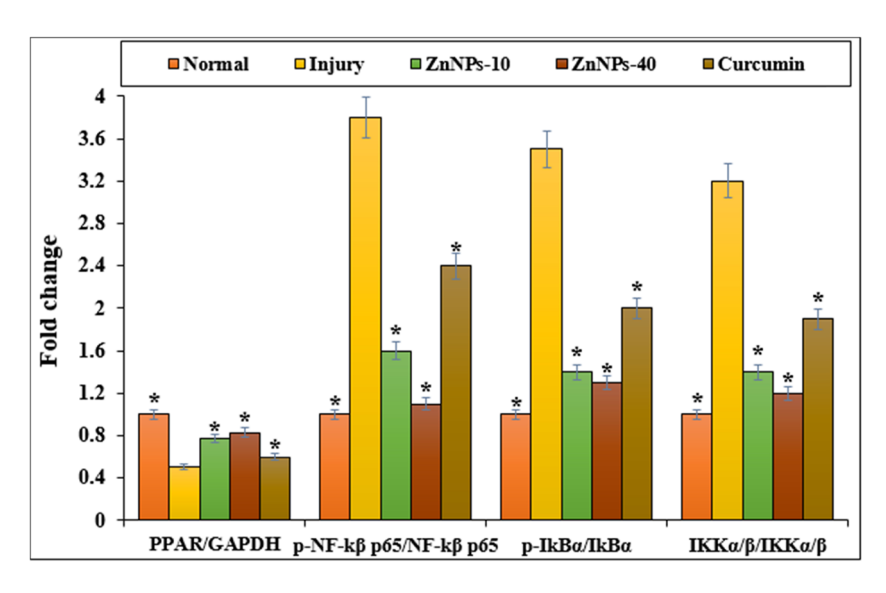


Figure 9: Effect of ZnNPs on several genes (fold change).

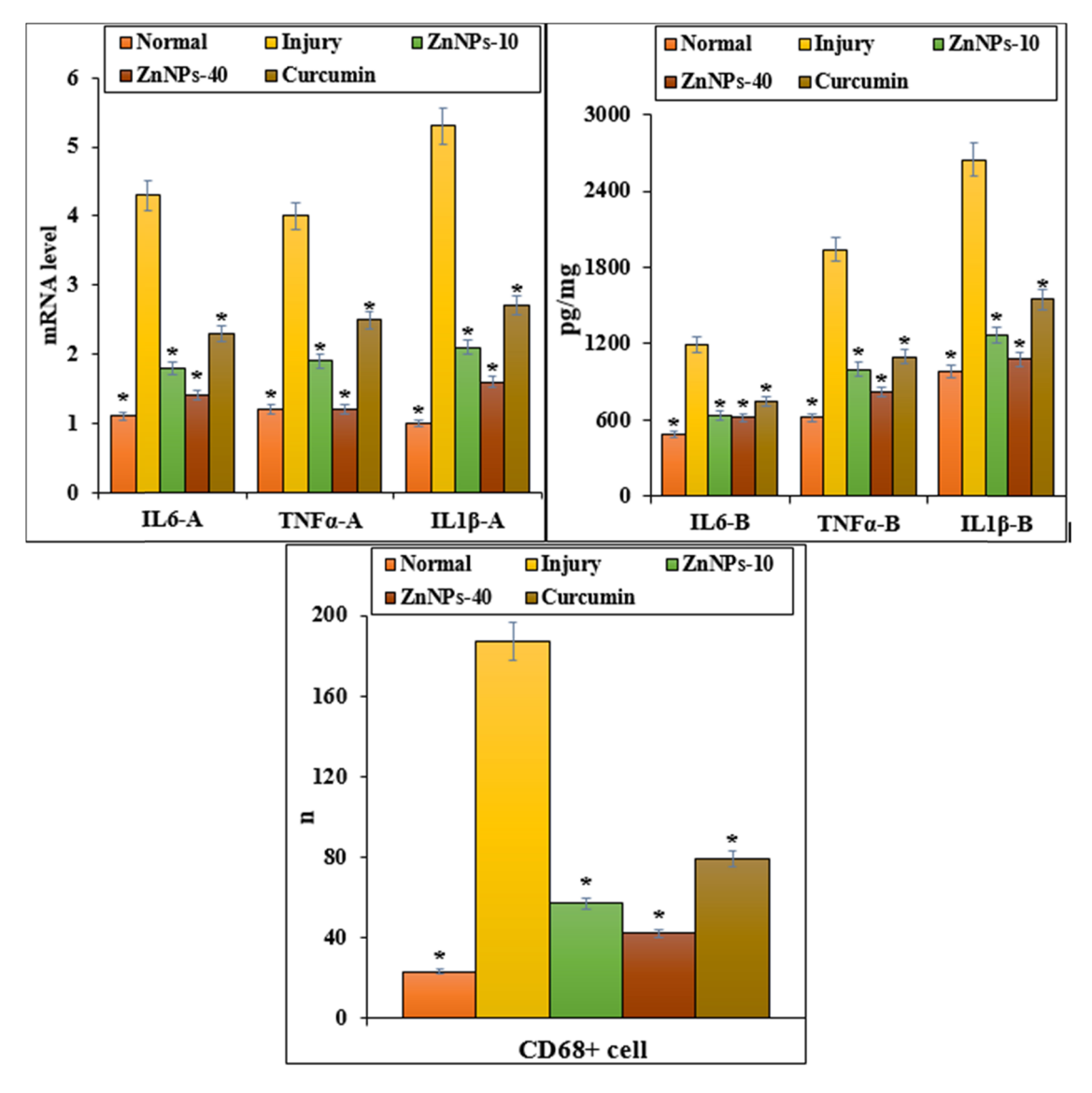


Figure 10: Effect of ZnNPs on the inflammatory cytokines mRNA levels (a), inflammatory cytokines quantitative analysis (b) pg/mg and CD68⁺ cell.

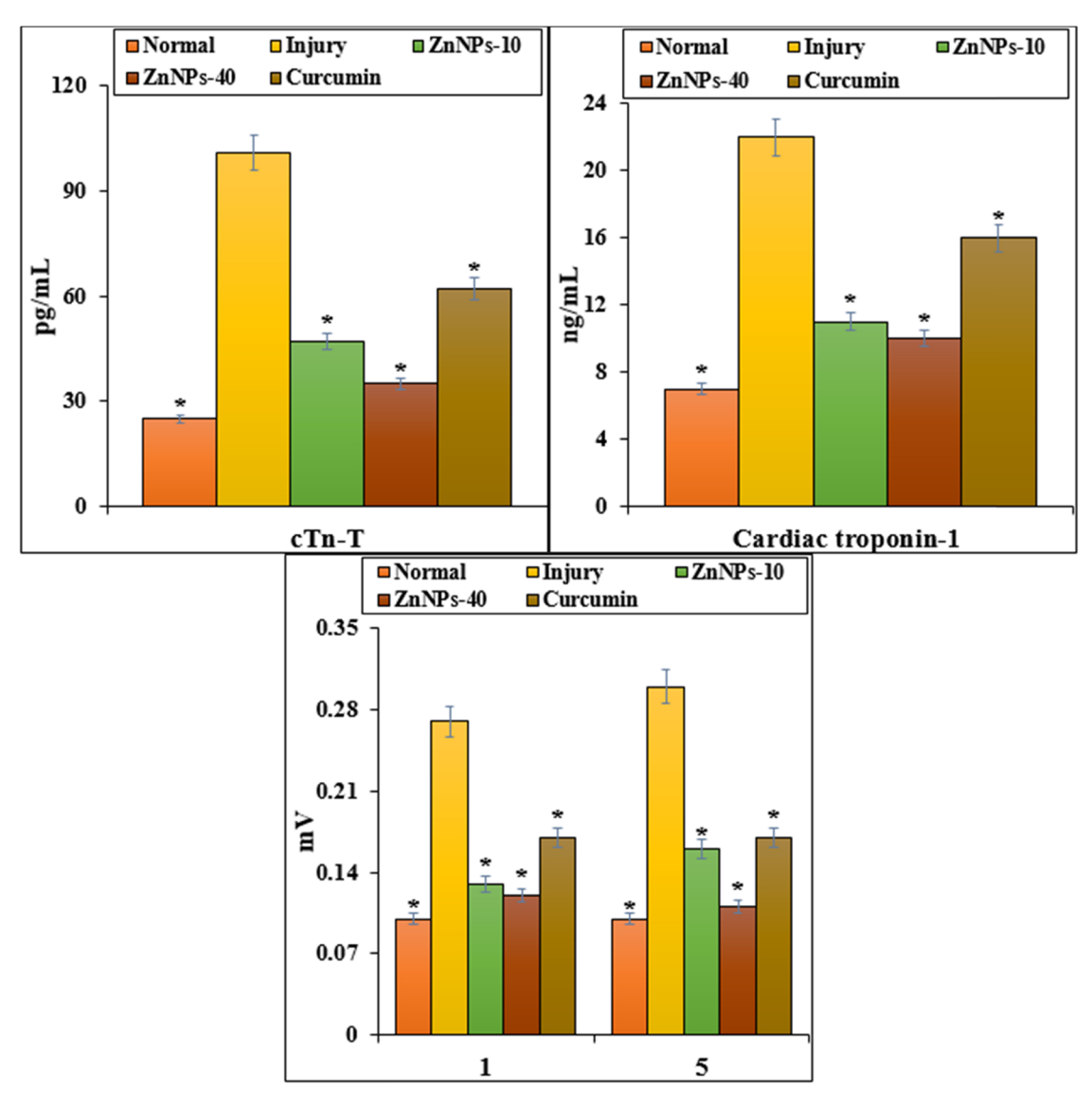


Figure 11: Effect of ZnNPs on the concentrations of cardiac troponin-1 (ng/mL) and cTn-T (pg/mL) and MI mice ST segment deviation (mV).

pathway and become active in response to external signals within the cell. Additionally, myocardial infarction triggers the inflammatory cytokines secretion and increases the activity of MAPK P38 [38]. Curcumin-synthesized nanoparticles show great promise in treating myocardial damage caused by isoproterenol intake. The nanoparticles possess antioxidant properties that, in conjunction with their compounds, have a significant effect on inhibiting 2,2-diphenyl-1-picrylhydrazyl free radicals. Boosting the immune system by increasing antioxidant levels undoubtedly protects individuals from chronic diseases. As stated by Martinez et al., antioxidants can reduce the likelihood of heart failure by affecting MAPK and kB-NF signaling pathways [39]. Therefore, the potential influence of curcumin-derived nanoparticles

on reducing MAPK expression may be due to their antioxidative traits.

The latest research revealed that the ZnNPs synthesized using curcumin led to a reduction in cardiac troponin-1, cTn-T, ST segment deviation in MI mice, as well as the heart wet weight/body weight ratio (Figures 11 and 12).

4 Conclusion

The author has effectively developed a cutting-edge drug for cardioprotection using ZnNPs combined with curcumin. This groundbreaking therapy is designed to combat

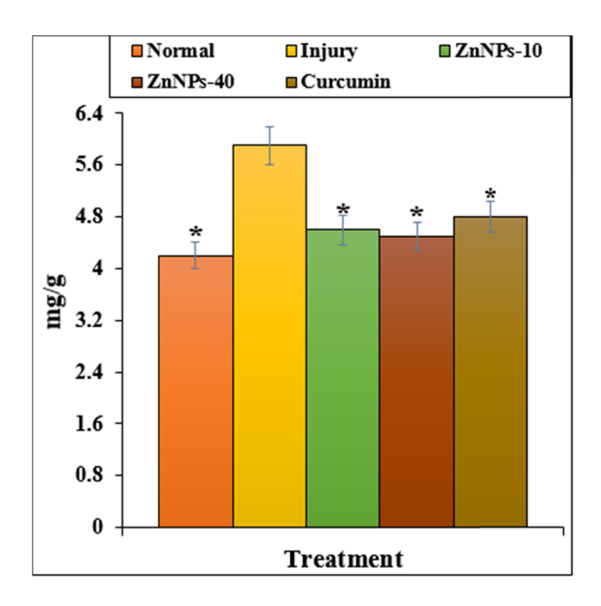


Figure 12: Effect of ZnNPs on heart wet weight/body weight ratio (mg/g).

isoproterenol-induced myocardial infarction in mice, with a particular emphasis on the PPAR- γ /NF- κ B pathway. The range of 400–700 cm⁻¹ showed vibrational bands for Zn–O bonds, as indicated by the FT-IR spectroscopy. Furthermore, the FE-SEM image exhibited a spherical morphology. ZnNPs have demonstrated the ability to reduce the pro-inflammatory cytokine levels in the hearts of mice with myocardial infarction. Moreover, they have been discovered to effectively suppress the myocardial injury marker levels, decrease mortality rates, and enhance ventricular wall infarction. The beneficial impacts of ZnNPs may be attributed to the normalization of gene expression associated with PPAR- γ /NF- κ B/I κ B- α /IKK α / β , and PPAR- γ phosphorylation.

Funding information: Author states no funding involved.

Author contributions: Lijuan Tan: conceptualization, data curation, formal analysis, acquisition, investigation, methodology, project administration, resources, software, supervision, validation, visualization, writing – original draft, and writing – review & editing.

Conflict of interest: There is no any conflict of interest.

Data availability statement: The datasets generated during and/or analyzed during the current study are available from the corresponding author upon reasonable request.

Ethical approval: The experiments were performed according to the ethical guidelines of the International Association for the Study of Humans.

References

- [1] Reed GW, Rossi JE, Cannon CP. Acute myocardial infarction. Lancet. 2017;389(10065):197–210.
- [2] Marín-Juez R, El-Sammak H, Helker CSM, Kamezaki A, Mullapuli ST, Bibli SI, et al. Coronary revascularization during heart regeneration is regulated by epicardial and endocardial cues and forms a scaffold for cardiomyocyte repopulation. Dev Cell. 2019;51(4):503–15.e4.
- [3] Rentrop KP, Feit F. Reperfusion therapy for acute myocardial infarction: concepts and controversies from inception to acceptance. Am Heart I. 2015;170(5):971–80.
- [4] Arbab-Zadeh A, Nakano M, Virmani R, Fuster V. Acute coronary events. Circulation. 2012;125(9):1147–56.
- [5] Ekroos K, Jänis M, Tarasov K, Hurme R, Laaksonen R. Lipidomics: a tool for studies of atherosclerosis. Curr Atheroscler Rep. 2010;12(4):273–81.
- [6] Young DR, Hivert MF, Alhassan S, Camhi SM, Ferguson JF, Katzmarzyk PT, et al. Sedentary behavior and cardiovascular morbidity and mortality: a science advisory from the American Heart Association. Circulation. 2016;134(13):e262–79.
- [7] Gorabi AM, Kiaie N, Reiner Ž, Carbone F, Montecucco F, Sahebkar A. The therapeutic potential of nanoparticles to reduce inflammation in atherosclerosis. Biomolecules. 2019;9(9):2545.
- [8] Ou LC, Zhong S, Ou JS, Tian JW. Application of targeted therapy strategies with nanomedicine delivery for atherosclerosis. Acta Pharmacol Sin. 2021;42(1):10–7.
- [9] Cervadoro A, Palomba R, Vergaro G, Cecchi R, Menichetti L, Decuzzi P, et al. Targeting inflammation with nanosized drug delivery platforms in cardiovascular diseases: immune cell modulation in atherosclerosis. Front Bioeng Biotechnol. 2018;6:177.
- [10] Bulgarelli A, Martins Dias AA, Caramelli B, Maranhão RC. Treatment with methotrexate inhibits atherogenesis in cholesterol-fed rabbits. J Cardiovasc Pharmacol. 2012;59(4):308–14.
- [11] Meneghini BC, Tavares ER, Guido MC, Tavoni TM, Stefani HA, Kalil-Filho R, et al. Lipid core nanoparticles as vehicle for docetaxel reduces atherosclerotic lesion, inflammation, cell death and proliferation in an atherosclerosis rabbit model. Vasc Pharmacol. 2019;115:46–54.
- [12] Zhang J, Zu Y, Dhanasekara CS, Li J, Wu D, Fan Z, et al. Detection and treatment of atherosclerosis using nanoparticles. Wiley Interdiscip Rev Nanomed Nanobiotechnol. 2017;9(1):e1412.
- [13] Dai W, Li Y, Liu X, Wang N, Luo P, Kong L. Protective effects of Nigella sativa L. seeds aqueous extract-based silver nanoparticles on sepsis-induced damages in rats. Inorg Chem Commun. 2024;166:112594.
- [14] Zhang D, Wang L, Tian L, Chen W, El-kott AF, Negm S, et al. Bioinspired deposition of gold nanoparticles onto the surface of kaolin for in vitro management of human ovarian cancer and modulation of the inflammatory response in adenomyosis-induced mice in vivo via the MAPK signaling pathway. J Sci: Adv Mater Devices. 2024;9(2):100714.
- [15] Guo Y, Shahriari M, Eltantawy W, El-kott AF, AlShehri MA, Ibrahim EH. Ultrasound assisted synthesis of starch-green tea extract composite and its therapeutic effects on adenomyosis by following the MAPK/ERK signaling and pro-inflammatory pathways in mice. J Polym Environ. 2024;1–10.
- [16] Bakir EM, Younis NS, Mohamed ME, El Semary NA. Cyanobacteria as nanogold factories: chemical and anti-myocardial infarction

- properties of gold nanoparticles synthesized by lyngbya majuscula. Mar Drugs. 2018;16:217.
- [17] Danila D, Johnson E, Kee P. CT imaging of myocardial scars with collagen-targeting gold nanoparticles. Nanomed Nanotechnol Biol Med. 2013;9:1067–76.
- [18] Shen Y, Gong S, Li J, Wang Y, Zhang X, Zheng H, et al. Co-loading antioxidant N-acetylcysteine attenuates cytotoxicity of iron oxide nanoparticles in hypoxia/reoxygenation cardiomyocytes. Int J Nanomed. 2019;14:6103–15.
- [19] Merinopoulos I, Gunawardena T, Stirrat C, Cameron D, Eccleshall SC, Dweck MR, et al. Diagnostic applications of ultrasmall superparamagnetic particles of iron oxide for imaging myocardial and vascular inflammation. JACC: Cardiovasc Imaging. 2021;14:1249–64.
- [20] Zheng H, You J, Yao X, Lu Q, Guo W, Shen Y. Superparamagnetic iron oxide nanoparticles promote ferroptosis of ischemic cardiomyocytes. J Cell Mol Med. 2020;24:11030–3.
- [21] Siddiqui SA, Or Rashid MM, Uddin MG, Robel FN, Hossain MS, Haque MA, et al. Biological efficacy of zinc oxide nanoparticles against diabetes: a preliminary study conducted in mice. Biosci Rep 40. 2020;40:BSR20193972.
- [22] Bashandy SA, Ahmed-Farid OA, Abdelmottaleb-Moussa S, Omara EA, Abdel Jaleel GA, Ibrahim FA. Efficacy of zinc oxide nanoparticles on hepatocellular carcinoma-induced biochemical and trace element alterations in rats. J Appl Pharm Sci. 2021;11:108–17.
- [23] Jain D, Shivani, Bhojiya AA, Singh H, Daima HK, Singh M, et al. Microbial fabrication of zinc oxide nanoparticles and evaluation of their antimicrobial and photocatalytic properties. Front Chem. 2020;8:778.
- [24] Ahmed RF, Nasr M, Abd Elbaset M, Hessin AF, Ahmed-Farid O, Shaffie NM, et al. Combating hematopoietic and hepatocellular abnormalities resulting from administration of cisplatin: role of liver targeted glycyrrhetinic acid nanoliposomes loaded with amino acids. Pharm Dev Technol. 2022;27:925–941. doi: 10.1080/10837450. 2022.2129687
- [25] El-Bahr SM, Shousha S, Albokhadaim I, Shehab A, Khattab W, Ahmed-Farid O, et al. Impact of dietary zinc oxide nanoparticles on selected serum biomarkers, lipid peroxidation and tissue gene expression of antioxidant enzymes and cytokines in Japanese quail. BMC Vet Res. 2020;16:349.
- [26] MacKenzie S, Bergdahl A. Zinc homeostasis in diabetes mellitus and vascular complications. Biomedicines. 2022;10:139.

- [27] Kambe T, Tsuji T, Hashimoto A, Itsumura N. The physiological, biochemical, and molecular roles of zinc transporters in zinc homeostasis and metabolism. Physiol Rev. 2015;95:749–84.
- [28] Huang X, Zheng X, Xu Z, Yi C. ZnO-based nanocarriers for drug delivery application: from passive to smart strategies. Int J Pharm. 2017;534:190–4.
- [29] DiSilvestro RA. Zinc in relation to diabetes and oxidative disease. I Nutr. 2000;130:15095–S1511.
- [30] Huang L, Teng T, Bian B, Yao W, Yu X, Wang Z, et al. Zinc levels in left ventricular hypertrophy. Biol Trace Elem Res. 2017;176:48–55.
- [31] Arozal W, Monayo ER, Barinda AJ, Perkasa DP, Soetikno V, Nafrialdi N, et al. Protective effects of silver nanoparticles in isoproterenol-induced myocardial infarction in rats. Front Med (Lausanne). 2022 Aug;9:867497.
- [32] Huang HB, Leung DYC, Kwong PCW, Xiong J, Zhang L. Enhanced photocatalytic degradation of methylene blue under vacuum ultraviolet irradiation. Catal Today. 2013;201:189–94.
- [33] Verma VK, Malik S, Narayanan SP, Mutneja E, Sahu AK, Bhatia J, et al. Role of MAPK/NF-κB pathway in cardioprotective effect of Morin in isoproterenol induced myocardial injury in rats. Mol Biol Rep. 2019;46(1):1139–48.
- [34] Ren G, Cui Y, Li W, Li F, Han X. Research on cardioprotective effect of irbesartan in rats with myocardial ischemia-reperfusion injury through MAPK-ERK signaling pathway. Eur Rev Med Pharmacol Sci. 2019;23(12):5487–94.
- [35] Liu K, Wang F, Wang S, Li W-N, Ye Q. Mangiferin attenuates myocardial ischemia-reperfusion injury via MAPK/Nrf-2/HO-1/NF-κB in vitro and in vivo. Oxid Med Cell Longev. 2019;2019;7285434.
- [36] Bao W, Hu E, Tao L, Boyce R, Mirabile R, Thudium DT, et al. Inhibition of Rho-kinase protects the heart against ischemia/ reperfusion injury. Cardiovasc Res. 2004;61(3):548–58.
- [37] Fakhri F, Shakeryan S, Fakhri S, Alizadeh A. The effect of 6 weeks of high intensity interval training (HIIT) with nano-curcumin supplementation on factors related to cardiovascular disease in inactive overweight girls. Feyz. 2020;24(2):181–9.
- [38] Krishnamurthy P, Rajasingh J, Lambers E, Qin G, Losordo DW, Kishore R. IL-10 inhibits inflammation and attenuates left ventricular remodeling after myocardial infarction via activation of STAT3 and suppression of HuR. Circ Res. 2009;104(2):e9–e18.
- [39] Martinez PF, Bonomo C, Guizoni DM, Junior SA, Damatto RL, Cezar MD, et al. Modulation of MAPK and NF-κB signaling pathways by antioxidant therapy in skeletal muscle of heart failure rats. Cell Physiol Biochem. 2016;39(1):371–84.